Engineering Structures 122 (2016) 62–71

Contents lists available at ScienceDirect

Engineering Structures

journal homepage: www.elsevier.com/locate/engstruct

Vibration suppression of cables using tuned inerter dampers

I.F. Lazar [a,*], S.A. Neild [a], D.J. Wagg [b]

[a] Department of Mechanical Engineering, University of Bristol, Bristol BS8 1TR, UK
[b] Department of Mechanical Engineering, University of Sheffield, Sheffield S1 3JD, UK

ARTICLE INFO

Article history:
Received 21 June 2015
Revised 6 April 2016
Accepted 7 April 2016
Available online 25 May 2016

Keywords:
Cable dynamics
Tuned inerter damper (TID)
Vibration suppression

ABSTRACT

This paper considers the use of a tuned inerter damper (TID) system for suppressing unwanted cable vibrations. The TID consists of an inerter, a device that exerts a force proportional to relative acceleration, coupled with a parallel spring and damper. It may be thought of as similar to a tuned-mass-damper, but requiring two terminals. As a two terminal device, the performance of the TID is compared to the classical use of viscous dampers (VD) located close to one of the cable supports. We show that the limitation that exists with VDs, where the modal damping of the cable cannot exceed a maximum level for a given damper location, can be overcome through the use of the TID at the same location. A practical design methodology, based on the minimisation of the displacement amplitude at the mid-span of the cable subjected to support excitation, is proposed. An example where a cable is subjected to the El-Centro earthquake demonstrates that the system's response is improved when a TID is used instead of a VD.

1. Introduction

Cables are widely used structural elements capable of bearing tensile forces. Cables experience vibration problems due to their very low damping. The problems associated with cable vibration are especially important for bridge design and retrofitting. Bridge cables are subject to vibrations induced by wind, wind-rain, traffic and earthquakes. These unwanted vibrations need to be reduced to acceptable levels. Irvine gives an overview of cable dynamics in [1]. More recently, Rega published a review on the nonlinear vibrations of suspended cables in [2,3].

In order to limit unwanted vibration in cable-stayed bridges, viscous dampers can be attached between the cables and the deck, near the anchorage point of each cable. Several studies have been made in order to understand the subsequent dynamic behaviour. Kovacs [4] was the first to define the concept of maximum attainable modal damping. Later, Yoneda & Maeda [5] proposed the use of a set of empirical equations for defining the optimum damper size and Uno et al. [6] introduced the use of non-dimensional damping coefficients. Later, Pacheco et al. [7] determined the universal curve for estimating the modal damping of stay cables and Krenk [8] gave an analytical formula for the universal curve, based on complex modes analysis. Then, Cremona [9] extended the universal curve formulation to inclined cables. Main and Jones [10] extended these studies to the case where the damper is installed further away from the support. There have been several case studies looking into the performance of bridges with attached viscous dampers [11], where their effectiveness has been demonstrated. Magneto-rheological (MR) dampers have also been considered as an alternative to viscous dampers [12–14].

However, it has been shown that there are limitations to the effectiveness of dampers mounted on cables because their installation is restricted to be near the end of the cable, generally at distances lower than 5% of the cable length, see for example [15]. Over this range, regardless of the damping coefficient, there is a maximum modal damping that can be achieved using a viscous damper [8]. This disadvantage may be overcome by the use of tuned mass dampers (TMD) that can be installed anywhere along the cable length, as they require no attachment to the ground or bridge deck [16]. Such systems have already been designed and tested.

A parametric study was conducted by Wu & Cai in [17] to quantify the influence of parameters such as TMD mass and damping ratio, cable inclination and TMD location on the system's performance. Casciati & Ubertini [18] extended the use of TMDs to the mitigation of spatial vibrations of shallow cables by adopting a variable inclination device attached to the cable.

Anderson et al. [19] made a comparison between cables with attached VDs and TMDs and assessed the performance of the two types of systems. It was shown that a TMD located at 40% distance from the support is more efficient than a damper located very close to the support. The clear disadvantage of the TMD option is the access issues at these locations.

* Corresponding author.
E-mail address: Irina.Lazar@bristol.ac.uk (I.F. Lazar).

http://dx.doi.org/10.1016/j.engstruct.2016.04.017
0141-0296/

The aim of this paper is to investigate whether an inerter-based system can be used to overcome the performance limitations of a VD while retaining its advantage that it is mounted close to the anchorage point and so it is easily accessible.

The inerter was originally designed by Smith [20] to complete the force-current analogy between mechanical and electrical networks. This is the equivalent of a capacitor and the force produced is proportional to the relative acceleration between the device terminals. The proportionality constant is called inertance and is measured in kilograms. Initially designed for Formula 1 racing car suspension systems, under the name of J-damper [21], the inerter is used today in vehicle [22–24], train [25] and building [26,27] suspension systems. The use of inerters for civil engineering applications has been extended to suppression systems in the form of tuned viscous mass dampers [28,29], tuned mass-damper-inerter systems [30] and tuned inerter dampers (TID) [31]. Unlike the mass in a TMD, the inerter can be geared such that the apparent mass is far higher than the actual mass of the device; gearing ratios of 200:1 have been achieved [28]. This offers the potential for much higher mass ratios than those feasible for TMDs [31].

In this paper, the authors propose the use of a TID system, where the traditional TMD mass is replaced by an inerter. A schematic diagram of the resulting system is shown in Fig. 1. The potential advantage of using a TID comes from the use of gearing in the inerter, allowing a much higher apparent mass then the mass of the device. For example, a commercially available inerter, the Penske 8760H, has an apparent mass (inertance) to device mass ratio of 38, with higher mass ratios available on demand. Therefore, it is feasible for the inerter's physical mass to remain low regardless of its inertance. This is in contrast to the mass in a TMD, which is generally limited to 10% of the host structure mass. As in the case of cables with attached dampers, the TID needs to be located next to the support (in the range of 0–5%), connected between the deck and the cable. This can be advantageous in terms of maintenance or for retrofitting.

The paper discusses the performance of VDs and, building on this, proposes an optimisation and tuning strategy for TIDs installed on cables. For a convenient design process, contour plots are proposed for both VD and TID systems. For VDs, the only tuning parameter is the device's damping coefficient and, based on the contours plots provided, the user can select the optimal damping ratio using the device location. For TIDs, there are three design parameters, namely the apparent mass ratio, the damping ratio and the frequency ratio (between the TID and the host structure). Therefore, after selecting the desired apparent mass ratio and the connection point location, the user is provided with two extra contour plots where the matching damping and frequency ratios can be identified. Hence, a practical design method that can be employed by the engineer for both VD and TID systems is provided, see Section 4.

To support the theoretical findings, a numerical application where a cable is subjected to sinusoidal and earthquake support excitation is presented in Section 5. It is shown that the performance of an optimal damper can be achieved by attaching a TID with a mass ratio of only 10% of the total cable mass. Moreover, while there is only one optimal damper that can be used in a certain connection point, the performance of a TID can be improved further by increasing its apparent mass ratio. This can be easily achieved in practice, given the inerter's capacity of generating high apparent masses [28,33].

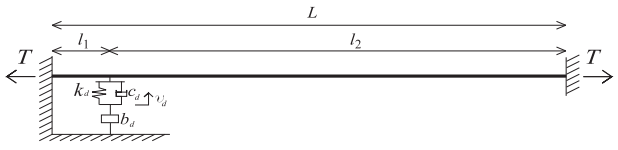

Fig. 1. Cable with attached TID.

2. Study of cables with attached dampers

Several numerical solutions have been proposed for the case when dampers are attached to cables, starting from the partial differential equation describing the cable vibration and by proposing different functions for the cable's mode shapes. Such algorithms are described in greater detail in [8] and [10]. However, the analysis of the TID is more complex due to the additional degree of freedom within the device. In order to reduce the computational effort necessary for numerically solving a system of partial differential equations, a finite element model of the cable was created using axial elements.

2.1. Finite element model

A 20 axial elements model of the cable was used. The accuracy of the model was validated against the analytical expressions for the combined cable-TID system using the approach reported for cable-damper systems in [8]. To accommodate the TID and VD when selecting the elements' lengths, the device-cable connection point was included as a node. For example, if the connection point is located at 1% distance from the support, the first element will have a length of 0.01L, the second element will have a length of 0.09L and the other elements will have the length 0.05L. As expected, this change will influence the natural frequency of the finite element modelled cable. However, the changes are very small and the impact on the overall response is arguably negligible (less than 0.1%).

Having chosen the number of elements, the mass and stiffness matrices are assembled for the simple cable. Since the VD does not alter the mass and stiffness of the cable, these matrices remain unchanged. The damping matrix changes, allowing for the added damping to be taken into account. When adding a TID, an additional degree of freedom is added to these matrices. All matrices are described in the Appendix at the end of the paper, along with the conversion of the resulting equation of motion into state space.

2.2. Performance analysis

The problem of cable vibration suppression by means of magneto-rheological (MR) or viscous dampers (VD) has been studied in-depth in the existing literature. The results presented in [8] prove the existence of an optimum set of parameters that need to be used in order to obtain the best performance of the cable plus damper system. By employing the optimal damping ratio corresponding to a given location of the damper, it can be ensured that the maximum amount of damping is transferred to the cable. This also translates into optimum performance in terms of maximum displacement amplitude. In the current study, the damping ratio is defined as

$$\xi_{VD} = \frac{c}{2\sqrt{Tm}} \tag{1}$$

where c represents the VD damping coefficient, T is the tension in the cable, and m is the cable mass per unit length.

Fig. 2(a) shows the modal damping ratios obtained in the first, second and third mode of the cable, when a damper is attached at 0.05L distance from the left support. It can be seen that, for all three modes, the maximum modal damping ratio is approximately $\zeta_1 = 2.7\%$, achieved for different device damping ratios, $\xi_{VD} = 3.2$ for mode 1, $\xi_{VD} = 1.6$ for mode 2 and $\xi_{VD} = 1.1$ for mode 3. This indicates that a device tuned to suppress vibration of the first

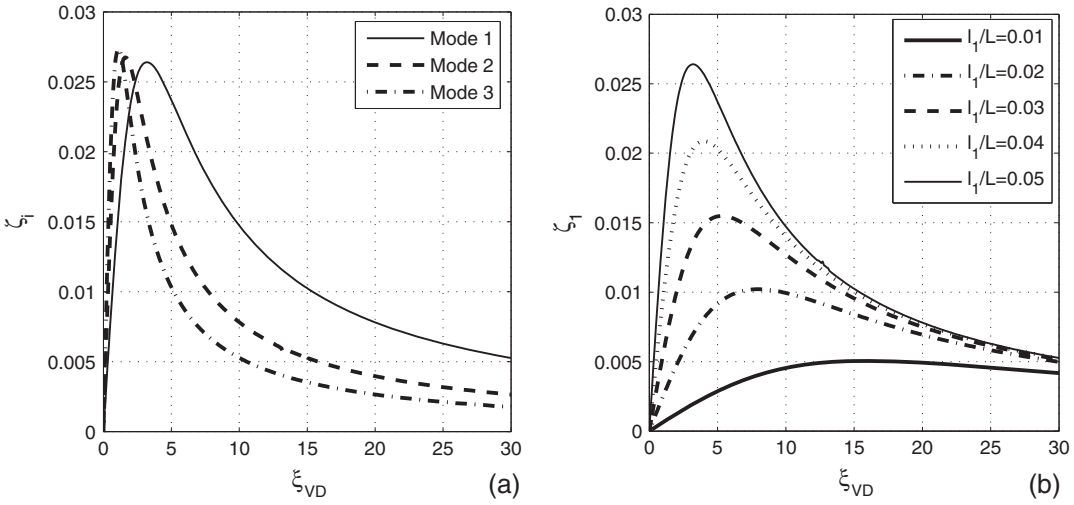

Fig. 2. (a) First, second and third modal damping ratio vs. VD damping ratio for a damper installed at 5% distance from the support and (b) first modal damping ratio vs. VD damping ratio for a damper installed at varying support distances situated between 1% and 5%.

mode will not be optimal in the upper modes of vibration. For example, by choosing $\xi_{VD} = 3.2$, we will achieve a modal damping ratio $\zeta_1 = 2.64\%$, but the resulting modal damping ratios for modes 2 and 3 will be $\zeta_2 = 2.03\%$ and $\zeta_3 = 1.5\%$ respectively. A similar plot is shown in [8], based on an asymptotic solution of the cable frequency equation. The results obtained here based on the finite element model match the ones in [8], where the scaling of the axes also causes the three curves corresponding to the first, second and third vibration mode to collapse. Here the axes are not scaled in order to allow the comparison with the TID case.

Fig. 2(b) shows the effect of varying the damping ratio of the VD device on the modal damping of the first vibration mode of the cable system, for a range of damper locations. The thin solid line corresponds to the solid line in Fig. 2(a). As the viscous damper is moved further from the support, the effect on the cable behaviour becomes more beneficial. Also, a higher optimal modal damping ratio is achieved with a smaller capacity damper when the device is moved away from the support.

Fig. 3 shows the relation between the optimal VD damping ratio (dashed line) and maximum modal damping ratio (thin solid line) of the cable for a varying length ratio, l_1/L. The maximum modal damping ratio that can be achieved using a VD increases approximately proportionally with the length ratio at which the damper is located. This ties in with the equation obtained for the optimal damping ratio in [8], which varies linearly with the length ratio

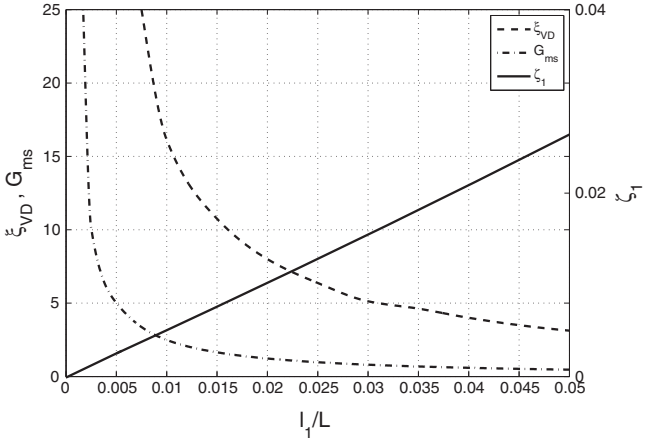

Fig. 3. Variation of the amplitude gain, G_{ms}, modal damping and VD damping ratio with the length ratio.

(Eq. 25 of [8]). As already noted, the optimal damping ratio for the damper, ξ_{VD}, reduces as the viscous damper is moved further from the left cable support.

In the case of VDs, the performance is directly related to the level of modal damping of the controlled cable. The displacement response is minimised when the modal damping ratio is maximised. Therefore, the modal damping ratio represents an accurate measure of the overall system performance. However, for TIDs, this does not suffice. Tuning the TID to obtain the maximum modal damping ratio of the targeted vibration mode of the cable does not imply that the corresponding cable response will be optimum (here, this is defined as the minimised displacement response at the cable's midspan). This is due to the additional degree-of-freedom and hence resonance, introduced by the presence of the device. Due to this, consideration should also be given to other parameters, such as the frequency ratio between the TID and the cable. This will be detailed in the following section.

Therefore, in order to be able to correctly assess and compare the performance of the TID and VD systems, a new performance parameter is introduced to asses the damper's performance, namely the displacement response gain between the support and the cable's midspan, when the cable is subjected to sinusoidal support excitation at both ends. As mentioned above, for the VD this will automatically mean that the maximum modal damping ratio is achieved.

The midspan gain is denoted by G_{ms} and offers an insightful measure of the damper performance when the design goal is to reduce the cable vibration amplitude that in the first mode of vibration is obtained at the midspan. The dash-dotted line in Fig. 3 represents the variation of the maximum amplitude gain, G_{ms}. As can be seen, the gain reduces when the length ratio is increased, but the rate of change with length reduces gradually. This indicates that positioning the device at a higher distance from the support will not bring significant improvement of the overall system response. The minimum gain obtained by installing a VD suppressor at 0.05% distance from the support is $G_{ms} = 0.47$.

3. Study of cables with attached tuned inerter dampers

3.1. Damping ratio definition

For a TID system, the device damping ratio (introduced in Section 2) is defined as

$$\xi = \frac{c_d}{2\omega_d b_d} \tag{2}$$

where c_d is the damping coefficient of the TID, ω_d is the TID natural frequency and b_d is the inertance.

For a VD, the damping ratio, defined by Eq. (1) for consistency with [8,10], is relative to the mass per unit length and tension in the cable. An equivalent damping ratio of the TID, relative to the cable is defined as

$$\hat{\xi}_{TID} = \xi \frac{\pi\mu}{\rho} \tag{3}$$

where ξ is the TID damping ratio defined in Eq. (2), μ is the inertance to cable mass ratio and ρ is the TID to cable natural frequency ratio. This new damping ratio definition is necessary in order to compare the performance of the two systems.

3.2. Tuning

When inerters are used to suppress vibrations in buildings, it was shown in [31] that the TID displays a TMD-like behaviour when excited in the vicinity of the first fundamental frequency of the host structure and a VD-like behaviour when excited at higher frequencies. This leads to the creation of two split peaks due to the introduction of an extra degree of freedom. If the primary structure is undamped (very lightly damped in practice), the tuning can be achieved using the fixed-point theory given by den Hartog [32]. It was also shown in [31] that in the case of TIDs, there exists a third fixed point, located at a high frequency, however this does not need to be taken into account in the tuning.

While in the case of dampers, the only tuning parameter that needs to be set is the device damping ratio, ξ_{VD}, in the TID case, the number of design parameters is increased to three, the mass ratio, μ, the device damping ratio, ξ and the frequency ratio, ρ.

Due to the two closely spaced modes, the tuning for a cable is optimised numerically, based on the minimisation of the displacement gain in the cable's midspan (G_{ms}), described in the previous section, leading to the creation of two equal amplitude split peaks. If we were to optimise the response by maximising the modal damping ratio of the first vibration mode of the controlled cable, we would obtain uneven split peaks, as the second mode would be less damped. Since for a TID the first two modes are closely spaced, the aim is for them to be equally damped. Otherwise, the frequency response would still be amplified at a frequency close to the first fundamental frequency of the uncontrolled cable.

Following the approach used in the Section 3, Fig. 4(a) shows the modal damping ratios obtained in the first, second and third mode of vibration of the cable, when a TID is attached at $0.05L$ distance from the support. Note that in the case of TIDs, this is not the maximum damping ratio that can potentially be achieved, but the damping ratio resulting from the optimisation of the midspan gain G_{ms} (as pointed out before, the maximum achievable modal damping ratio and the optimal modal damping ratio have different values for the TID).

These results were obtained for an apparent mass ratio of $\mu = 0.5$. This apparent mass ratio may seem high if one compares to traditional mass-based vibration absorbers, such as TMDs. However, it must be emphasised that μ is the ratio between the inerter's apparent mass (known as inertance) and the host structure mass. The actual mass of the inerter is much less than the apparent mass due to gearing. Taking the commercially available 38:1 gearing, the device mass to cable mass ratio is 1.3%, which would typically be much lower than that used for a TMD.

For each device damping ratio considered, the optimum frequency (and hence device spring stiffness) is calculated following the approach described earlier. In contrast with the VD suppressor, when using a TID we obtain significantly different damping ratio peaks for the first three vibration modes. Therefore, when the TID is tuned to suppress the vibration of the first mode, the system will be less efficient in the second and third modes. However, the maximum damping ratio achieved in the first mode is significantly larger, $\zeta_1 = 6.3\%$ (peak of the thin solid lines in Fig. 4(a) and (b)), compared with the case of a VD where the maximum value attained is $\zeta_1 = 2.6\%$ (peak of the thin solid lines in Fig. 2(a) and (b)).

We can obtain a family of curves corresponding to different length ratios while keeping the mass ratio constant at $\mu = 0.5$. The resulting curves are shown in Fig. 4(b). When the TID is moved further away from the support, a higher modal damping ratio can be achieved. However, this is done at the expense of a larger TID damping ratio, $\hat{\xi}_{TID}$. It is important to notice that the device damping ratios necessary to achieve the optimal modal damping ratio are much higher in the case of VD suppressors than for TID

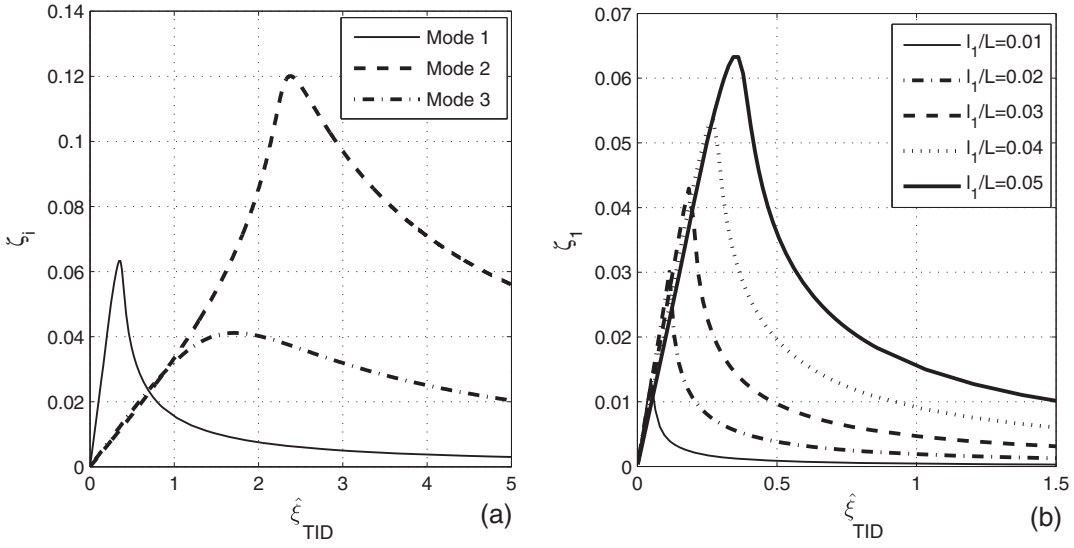

Fig. 4. (a) First, second and third modal damping ratio vs. TID damping ratio for a TID installed at 5% distance from the support using for each $\hat{\xi}_{TID}$ value the optimal ρ to minimise G_{ms} about the first cable mode and (b) first modal damping ratio vs. TID damping ratio for a TID installed at varying support distances situated between 1% and 5%, again using for each $\hat{\xi}_{TID}$ value the optimal ρ to minimise G_{ms} about the first cable mode.

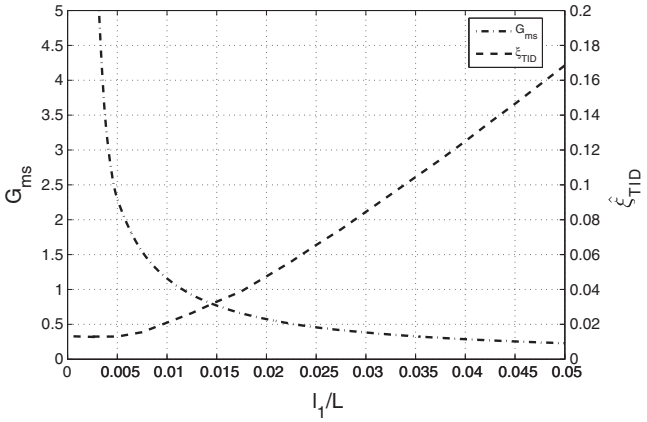

Fig. 5. Variation of the cable midspan gain and of the TID damping ratio with the length ratio.

suppressors, turning the TID into an economical alternative to the use of VDs.

Fig. 5 represents the TID suppressor equivalent of Fig. 3, namely the optimally tuned performance of the TID suppressor as a function of device location for the case when $\mu = 0.5$. By comparing these results with those in Fig. 3 for the VD suppressor, it can be seen that better suppression (lower gain values, G_{ms}) can be attained for smaller device damping ratios. At $0.05L$, the gain reduces to a value of approximately 0.24, less than half of the one obtained by using an optimally tuned VD suppressor. The curve corresponding to the variation of the damping ratio achieved in the first mode of vibration, ζ_1, with the length ratio is not shown as this does not offer a good measure of the TID performance, as stated before. Note that the corresponding device stiffness (which has been optimised as a function of the length ratio l_1/L) is not shown, this will be addressed later.

Applying the same strategy for different mass ratios, we can find the optimum design point that leads to the minimum gain for a certain length ratio, l_1/L. Fig. 6 shows a comparison between the optimum performance of TID and VD suppressors. Note that interpolation was used to obtain smoother curves. The viscous damper optimum points correspond to the maxima in Fig. 2(b). In the case of the TID system, plots similar to Fig. 4(a) were obtained for several mass ratios, $\mu = (0.05, 0.1, 0.2, 0.5, 1)$. These results showed that the effective mass required to achieve the viscous damper performance is close to 10% of the total cable mass, over the length ratio considered. The TID performance increases with mass ratio, but the increase in performance becomes smaller. If the mass is increased beyond a certain threshold (approximately $\mu = 2$), the performance of the system stagnates. However, it is likely that such high mass ratio values are not practical. Most importantly, by varying the mass ratio, we can design a TID suppressor with better performance than any VD suppressor installed at the same location.

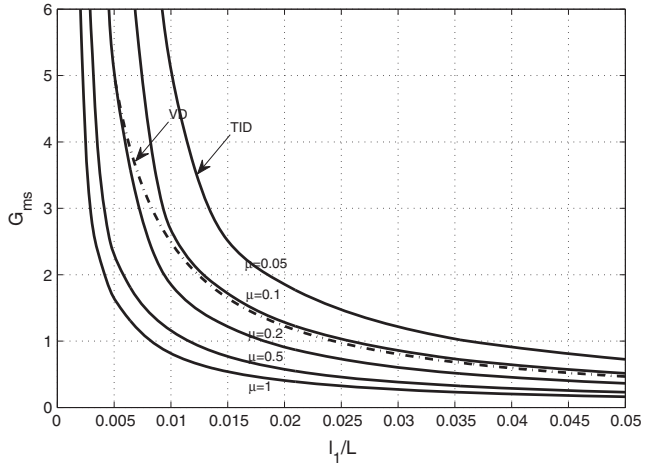

Fig. 6. Variation of the amplitude gain, G_{ms}, with length ratio, for TID and viscous damper systems.

Given these observations, a simplified design methodology that can easily be applied in practice, is now introduced. The following section proposes a tuning strategy based on contour plots, from which all design parameters can be selected.

4. Design methodology using contour plots

Following the idea of comparison between the two types of suppression systems studied, VDs and TIDs, performance contour plots have been generated in both cases. The contour plots present a practical parameter selection design method for the cases where a VD or a TID is attached to a cable.

4.1. Design of cables with attached VD suppressors

In the case of a cable with an attached VD suppressor, the choice of a suitably sized device is made based on the location of the VD and its damping ratio. The goal is to achieve the maximum level of damping in the first mode of vibration, ζ_1, and, as a result, the minimum amplitude gain G_{ms}. The curves in Fig. 7(a) represent constant levels of amplitude gain, when the cable is subjected to support excitation. Similarly, the curves in Fig. 7(b) represent constant levels of maximum damping ratio attained in the first mode of vibration of the cable and damper system. Looking at Fig. 7(b), it can be seen that regardless of the damper size, the maximum amount of damping that can be achieved is just above 2.5%, over the range $0 \leqslant l_1/L \leqslant 0.05$. Also, the shape of the curves reveals that increasing the damper capacity does not indefinitely improve the overall system behaviour. For example, if we connect a VD at a distance $l_1 = 0.02L$ from the support and want to achieve $\zeta_1 = 1\%$ damping in the first mode of vibration, we should employ a VD damping ratio situated in the interval $(6, 10)$. A further increase in VD damping would be detrimental to the overall system performance. The same observation applies in the case of Fig. 7(a). We can also note that the minimum gain that can be obtained is situated just below $G_{ms} = 0.5$, when a VD is located at 5% distance from the support. In fact, the plots shown in Fig. 2(b) represent vertical slices through 3D versions of Fig. 7(b).

The dashed line in Fig. 7(a) and (b) represents the locus of all optimal design points for a given length ratio. These are equivalent to the ξ_{VD} and G_{ms} curves in Fig. 3.

4.2. Design of cables with attached tuned inerter dampers

The same approach is applied to a cable with an attached TID. In this case, the number of design parameters is increased as the inertance-to-cable mass ratio, the damping ratio and frequency ratio of the TID play an important role in the overall system performance. The choice of parameters will be done in two steps. Firstly, using the amplitude gain contour plot shown in Fig. 8, we will choose the mass and length ratios necessary to achieve the desired gain. This step is similar to the procedure presented in the previous subsection. Secondly, using the contour plots in Fig. 9(a) and (b), we select the corresponding optimal TID frequency and damping ratio respectively (based on the length and mass ratios chosen in the previous step).

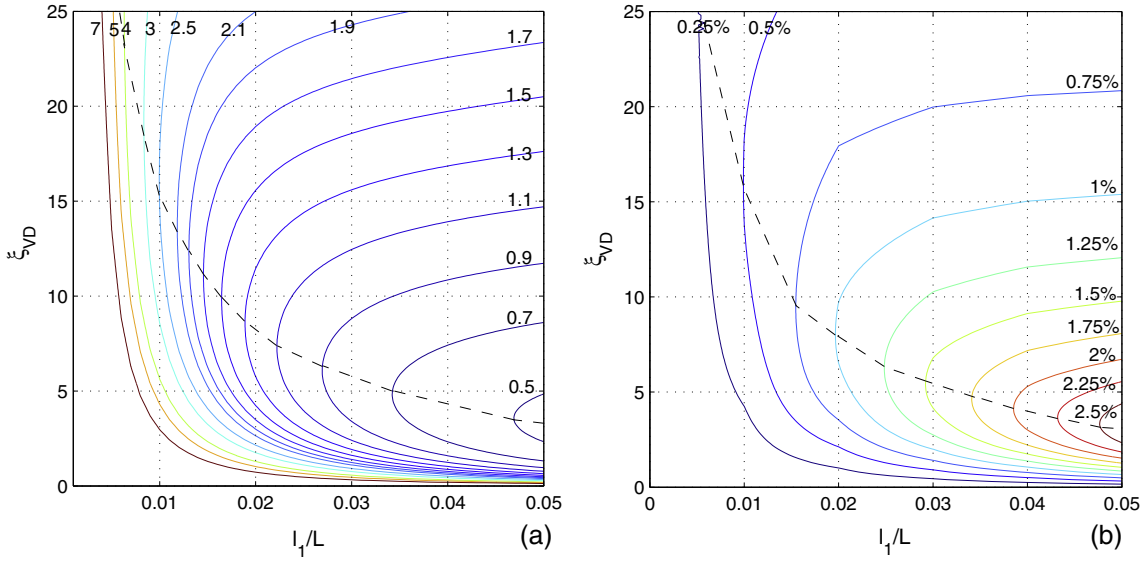

Fig. 7. (a) Cable maximum midspan displacement gain, G_{ms} contours as a function of VD damping ratio and length ratio and (b) cable modal damping ratio, ζ_1, contours as a function of VD damping ratio and length ratio.

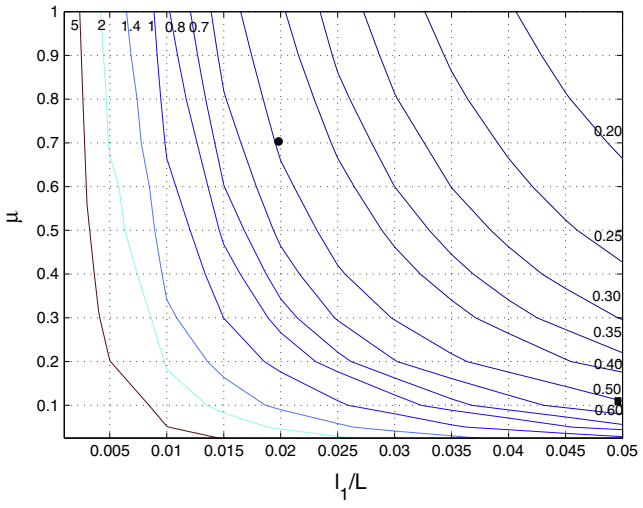

Fig. 8. Maximum midspan gain contours as a function of TID mass and length ratios.

For example, if we want to obtain the minimum gain that can be achieved with a VD, namely $G_{ms} = 0.5$ (from Fig. 7(a)), we need to place the VD at a distance $l_1 = 0.05L$ from the support. If a TID is connected instead, the same performance can be reached by using different mass ratio suppressors at certain locations. For instance, if the TID is connected at a distance $l_1 = 0.02L$ from the support, we need a mass ratio $\mu = 0.7$ to obtain a gain $G_{ms} = 0.5$ (◉ in the figure). If however the TID is connected at a distance $l_1 = 0.05L$, we need a mass ratio of only $\mu = 0.1$ (point ■ in the figure). The exact values can be calculated by interpolation based on the curves shown in the graphs. At the same time, it can be seen in Fig. 8 that the minimum gain that can be achieved using a TID is situated bellow $G_{ms} = 0.2$, less than half of the minimum gain obtained with a VD suppressor.

Then, for each case, Fig. 9(a) and (b) can be used to select the corresponding frequency and damping ratios. For a TID with mass ratio $\mu = 0.7$, located at a distance $l_1 = 0.02L$, the TID frequency ratio has to be set to $\rho = 0.94$ (Fig. 9(a)) and the damping ratio has to be set to $\xi = 12\%$ (Fig. 9(b)). For a TID with mass ratio $\mu = 0.1$, located at a distance $l_1 = 0.05L$, the TID frequency ratio has to be set to $\rho = 0.98$ (Fig. 9(a)) and the damping ratio has to be set to $\xi = 1.5\%$ (Fig. 9(b)). Note that the TID damping values are significantly lower than the VD ones, due to the use of the inerter.

The contour lines trend in Fig. 8 shows that if the TID mass ratio is increased, the gain of the overall system continues to decrease. However, as pointed out in the previous sections, if the mass ratio is increased past a certain threshold, the system's performance decreases, just as observed in the case of VD suppressors that have an optimal damping value (for a given location) beyond which its suppression capabilities decrease.

The results presented so far are now used to design a suppression device for an example system, following these steps:

STEP 1 The designer selects the desired vibration suppression level. For example, the cable vibration amplitude at midspan is to be reduced to half of that at the support. This means that the target midspan gain is set to 0.5.

STEP 2 Once the midspan gain has been established, the contour plot relating the midspan gain to the length and mass ratios (Fig. 8) is considered. On a case to case basis, various constraints may arise in terms of mass or length ratio. However, as long as the point of coordinates $(\mu, l_1/L)$ remains on the $G_{ms} = 0.5$ contour, the desired performance can be achieved.

STEP 3 The selected $(\mu, l_1/L)$ pair can now be mapped onto the contour plot relating it to the optimum frequency ratio (Fig. 9(a)). This allows the required TID spring stiffness, k_d, to be evaluated.

STEP 4 Lastly, the $(\mu, l_1/L)$ pair selected in STEP 2 is mapped onto the contour plots relating it to the optimum damping ratio (Fig. 9(b)). This leads the designer to the optimal TID damper size, c_d.

All TID components have now been sized to obtain the design requirements. The following section presents a numerical application, where the steps presented above are followed.

5. Numerical application

This section studies the performance of a cable with an attached viscous damper or TID.

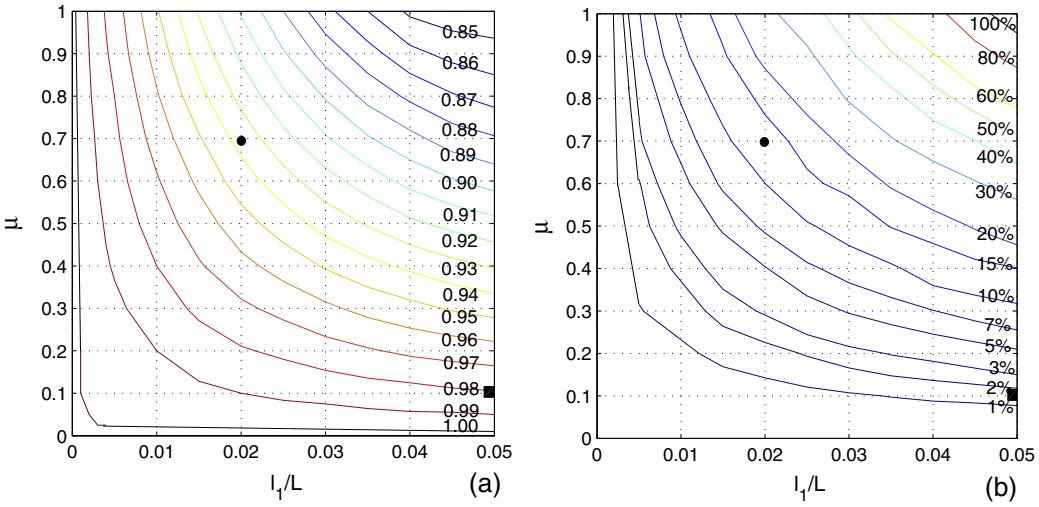

Fig. 9. (a) Optimal cable-to-TID frequency ratio contours as a function of TID mass ratio and length ratio and (b) optimal TID damping ratio (ξ) contours as a function of TID mass ratio and length ratio.

5.1. Cable model

For the application, we will consider the cable discussed in [16]. The cable length is $L = 93$ m, the static tension in the cable is $T = 5017$ kN and the mass per unit length is $m = 114.09$ kg/m. This leads to a fundamental frequency of $\omega_c = 7.084$ rad/s. The finite element model leads to a fundamental frequency of $\omega_c = 7.091$ rad/s for the first mode, equating to a percentage error of approximately 0.1%.

5.2. Study of the frequency response

The suppressors were tuned based on the contour plots described in the previous section (Fig. 7 for the VD suppressor and Figs. 8 and 9 for the TID suppressor). If we choose a viscous damper located at $l_1/L = 5\%$, by looking at Fig. 7(a), we can see that the optimal gain is obtained for a VD damping ratio of $\xi_{VD} = 2.35$. By analysing Fig. 7(b), we find that the maximum (and optimum) damping achieved in the first mode of vibration is a little bigger than $\zeta_1 = 2.5\%$. If we choose an equivalent TID (to get the same gain, G_{ms}), based on Fig. 8, we obtain a mass ratio of $\mu = 10\%$. Then, from Fig. 9(a) and (b), we can look up the optimum values for the frequency ratio and TID damping ratio, $\rho = 0.98$ and $\xi = 1.5\%$ (or $\hat{\xi}_{TID} = 0.5\%$) respectively.

Fig. 10 shows the frequency response of a selection of different damper and TID controlled systems, when the devices are located at a distance $l_1 = 5\%L$ from the support. While there is only one optimal damper that can be designed and used in this particular situation, in the case of TIDs, improved performance can be achieved by increasing the mass ratio beyond the level equivalent to the optimal VD suppressor, namely $\mu = 0.1$. The plot shows the frequency response corresponding to four other optimally tuned TID systems, for $\mu = 0.5, \mu = 0.7, \mu = 2$ and $\mu = 2.2$. Using $\mu = 0.5$ and $\mu = 0.7$ shows improved performance, the maximum gain being decreased by approximately 50%, from $G_{ms} = 0.5$ to $G_{ms} = 0.23$ and $G_{ms} = 0.2$ respectively. Also, the frequencies of the resulting split peaks become well separated. As stated before, there is a limit to this improvement, occurring at $\mu = 2$, beyond which increasing μ becomes ineffective. For example, it can be seen in the plot that if the mass ratio is increased from $\mu = 2$ to $\mu = 2.2$, the TID performance does not improve. Moreover, the damping and frequency ratios become very high.

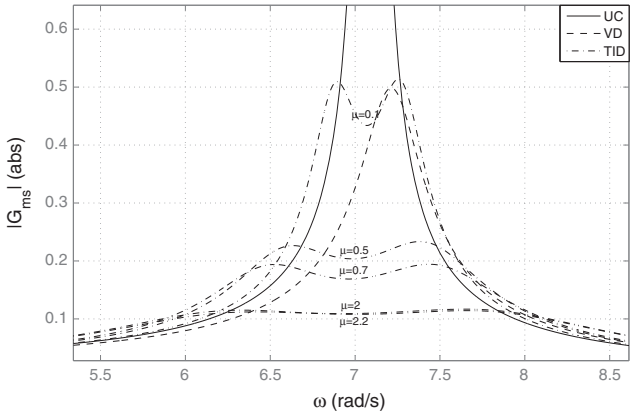

Fig. 10. Frequency response for TID and viscous damper systems located at 5% distance from the support. UC – uncontrolled cable response.

5.3. Earthquake excitation

This subsection is concerned with testing the newly developed system when it is used to control earthquake-excited cables. For this purpose, we have used a recording of the El-Centro earthquake, whose frequency content matches the natural frequencies of the structure. We considered the case when the uncontrolled cable is assumed to have no inherent damping. As a measure of the system's performance we have chosen the displacement at the midspan.

Fig. 11(a) shows the displacement time history at midspan, x_{ms}, for an uncontrolled cable, a cable with an attached VD designed at its optimal capacity, and a cable with an attached TID. For the latter, we chose two cases, one with performance similar to the optimal damper leading to a mass ratio of $\mu = 0.1$ and one with a mass ratio of $\mu = 0.5$. As expected, the displacement responses of the damper and lower mass TID controlled systems are nearly identical. However, while it is not possible to improve the viscous damper performance (for a given location), we can obtain an improved structural response of the TID controlled system by increasing its mass ratio and retuning the frequency and damping ratios according to the contour plots shown in Figs. 8 and 9.

For a better understanding of the system's behaviour, Fig. 11(b) shows the Fourier spectra of the same systems. As can be seen, the responses of the damper and lower mass TID-controlled systems are nearly identical in the vicinity of the fundamental frequency

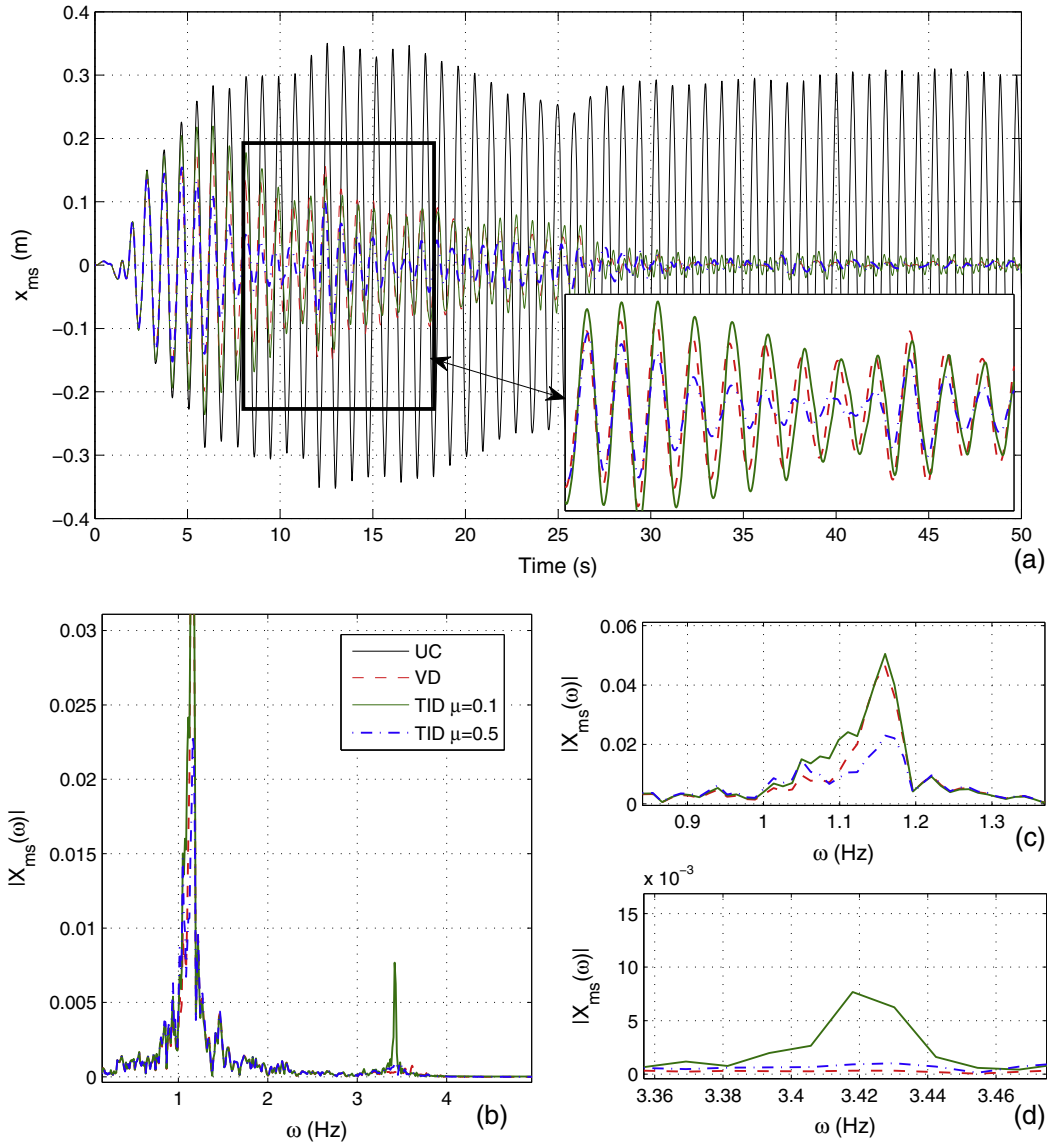

Fig. 11. (a) Time history of midspan displacement; (b) fourier spectrum of midspan displacement; (c) first frequency zoom-in and (d) second frequency zoom-in for a cable subjected to El-Centro earthquake.

of the cable, while the higher mass ratio TID is superior (Fig. 11(c)). The higher mass TID-controlled system shows a reduced amplitude at high frequencies as well, behaving similarly to the VD suppressor (Fig. 11(d)).

6. Conclusion

This paper proposed the use of tuned inerter dampers for cable vibration suppression, with the TIDs located in the vicinity of the cable support, as an alternative to the use of dampers.

TIDs offer a promising alternative to TMDs due to the fact that inerters, which generate a force proportional to the relative acceleration, are geared and can generate a far larger apparent mass than the actual device mass; ratios of 200:1 have been reported. The performance of the newly proposed device was assessed in comparison to that of a viscous damper connected at the same location. While the VD suppressor had only one design parameter (namely its damping), the TID performance depends on its mass ratio, frequency ratio (relatively to the fundamental frequency of the cable) and damping ratio. Based on the universal curves for estimation of modal damping, it has been concluded in previous research and also shown here that there is a maximum level of modal damping that can be achieved when a viscous damper is connected to a cable at a given location. However, the performance of a TID can be improved by the variation of its mass ratio, leading to very good vibration suppression levels.

Finally, a design methodology based on contour plots, aimed at choosing the optimal VD or TID suppressor to be connected at a given location along the cable length was proposed. Using this approach, the performances of equivalent VD and TID systems were shown. Then, improved results were obtained using a TID with a greater mass ratio, both in terms of frequency response and midspan displacement response when subject to earthquake loads. Considering the results shown, it was concluded that the TID represents a viable alternative to VDs when used to limit unwanted cable vibration.

Acknowledgements

I.F. Lazar is funded by a University of Bristol studentship. S.A. Neild is funded by an EPSRC fellowship EP/K005375/1. D.J. Wagg is supported by an EPSRC Grant EP/K003836/2. The authors gratefully acknowledge this funding.

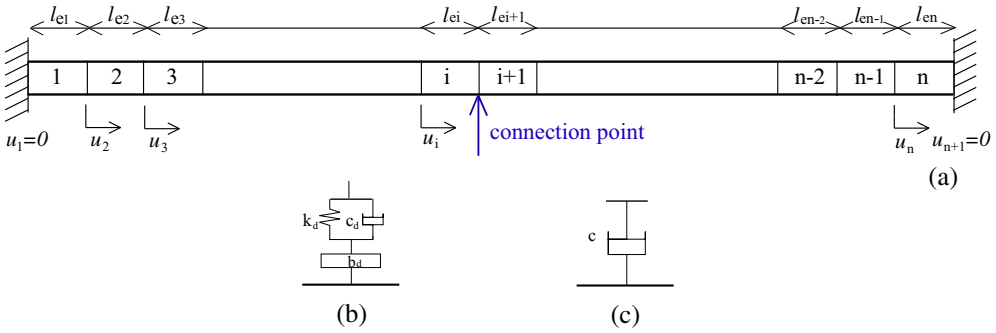

Fig. 12. (a) Finite element model of the cable, (b) TID and (c) VD.

Appendix A. Finite element model of the cable

In order to reduce the computational effort necessary for solving large systems of differential equations repeatedly, a finite element model of the cable was created using axial elements, as mentioned in Section 2.

The vertical motion of the cable in governed by the one-dimensional wave equation $\frac{\partial^2 u}{\partial t^2} = c^2 \frac{\partial^2 u}{\partial x^2}$, where $c = \sqrt{T/m}$ (T is the tension in the cable and m is the mass per unit length). This is identical to the axial vibration of a beam, albeit with $c = \sqrt{E/m}$ (E is the Young's modulus). Therefore, the FE model can be generated using the same, well documented, approach as a beam element axial vibration model, see for example [34] or [35]. The model is represented schematically in Fig. 12(a).

The local mass and stiffness matrices are given by

$$M_{ti} = \frac{m_i}{6}\begin{bmatrix} 2 & 1 \\ 1 & 2 \end{bmatrix} \quad \text{and} \quad K_{ti} = \frac{T}{l_{ei}}\begin{bmatrix} 1 & -1 \\ -1 & 1 \end{bmatrix} \tag{4}$$

where $m_i = ml_{ei}$ is the mass of element i. These, along with the boundary conditions (the cable is fixed at both ends), can be used to assemble the mass and stiffness matrices of the cable.

Considering a 4 elements cable, the mass and stiffness matrices of the uncontrolled cable become

$$\mathbf{M} = \frac{1}{6}\begin{bmatrix} 2m_1+2m_2 & m_2 & 0 \\ m_2 & 2m_2+2m_3 & m_3 \\ 0 & m_3 & 2m_3+2m_4 \end{bmatrix} \text{and} \quad \mathbf{K} = \begin{bmatrix} k_1+k_2 & -k_2 & 0 \\ -k_2 & k_2+k_3 & -k_3 \\ 0 & -k_3 & k_3+k_4 \end{bmatrix} \tag{5}$$

It is considered that the uncontrolled cable is undamped. Hence the damping matrix, $\mathbf{C} = O_{3,3}$, is a square null matrix. When a VD is attached to the cable, a single element of is modified, namely the one corresponding to the connection point of the VD. The mass and stiffness matrices remain unchanged. If a TID is connected, all matrices are modified, to accommodate the TID inertance, stiffness and damping. Moreover, the matrices' size increases by one, given the extra degree of freedom. The TID will always be connected between the cable and the deck. Say the connection point is between elements i and $i+1$, as in Fig. 12, for $n = 4$ and $i = 1$ (the TID is connected between the first and second element). Then, the cable plus TID system matrices become

$$\mathbf{M} = \frac{1}{6}\begin{bmatrix} 2m_1+2m_2 & m_2 & 0 & 0 \\ m_2 & 2m_2+2m_3 & m_3 & 0 \\ 0 & m_3 & 2m_3+2m_4 & 0 \\ 0 & 0 & 0 & b_d \end{bmatrix} \text{and} \quad \mathbf{K} = \begin{bmatrix} k_1+k_2+k_d & -k_2 & 0 & -k_d \\ -k_2 & k_2+k_3 & -k_3 & 0 \\ 0 & -k_3 & k_3+k_4 & 0 \\ -k_d & 0 & 0 & k_d \end{bmatrix} \tag{6}$$

The damping matrix is modified in a similar way to the stiffness matrix. Based on these matrices, we can write the equation of motion of the cable subjected to support excitation as

$$\mathbf{M}\ddot{x}(t) + \mathbf{C}(t)\dot{x} + \mathbf{K}x(t) = -\mathbf{M}\mathbf{J}r(t) \tag{7}$$

where $x(t)$ is the relative displacements vector, $r(t)$ is the support acceleration time history and $\mathbf{J}$ is a vector showing the distribution of the excitation across the structure. Eq. (7) can be translated into state space as

$$\dot{z}(t) = Az(t) + Br(t) \tag{8}$$

where

$$z(t) = \begin{bmatrix} x(t) \\ \dot{x}(t) \end{bmatrix}, A = \begin{bmatrix} I_{n,n} & O_{n,n} \\ -\mathbf{M}^{-1}\mathbf{K} & -\mathbf{M}^{-1}\mathbf{C} \end{bmatrix} \quad \text{and} \quad B = \begin{bmatrix} O_{n,1} \\ -\mathbf{J} \end{bmatrix} \tag{9}$$

where I and O are the identity and zero matrices respectively and n is the number of degrees-of-freedom of the system, given by the number of finite elements used and the type of device attached to the cable. The formulation above can be used to find the response of any of the proposed systems (cable, cable plus VD or cable plus TID). In each case, the mass, stiffness and damping matrices need to be updated accordingly. Note that the applications presented refer to ground excitation. Therefore, when assembling the vector J, we consider that the excitation is applied at both ends of the cable and at the connection of the TID/VD to the deck.

References

[1] Irvine HM. Cable structures. MIT Press; 1981.
[2] Rega G. Nonlinear vibrations of suspended cables – Part I: Modeling and analysis. ASME J Appl Mech Rev 2004;57(6):443–78.
[3] Rega G. Nonlinear vibrations of suspended cables – Part II: Deterministic phenomena. ASME J Appl Mech Rev 2004;57(6):479–514.
[4] Kovacs I. Zur Frage der Seilschwingungen und der Seildampfung. Bautechnik 1982;10:325–32.
[5] Yoneda M, Maeda K. A study on practical estimation method for structural damping of stay cable with damper. In: Proceedings of Canada–Japan workshop on bridge aerodynamics, Canada. p. 119–28.
[6] Uno K, Kitagawa S, Tsutsumi H, Inoue A, Nakaya S. A simple method of designing cable vibration dampers of cable-stayed bridges. J Struct Eng 1991;37:789–98.
[7] Pacheco BM, Fujino Y, Sulek A. Estimation curve for modal damping in stay cables with viscous damping. J Struct Eng 1993;119(6):1961–79.
[8] Krenk S. Vibrations of a taut cable with an external damper. J Appl Mech 2000;67:772–6.
[9] Cremona C. Courbe universelle pour le dimensinnement d'amortisseurs en pied de haubans. Revue Francaise du Genie Civil 1997.
[10] Main JA, Jones NP. Free vibrations of a taut cable with attached damper. I: Linear viscous damper. J Eng Mech 2002;128:1062–71.
[11] Main JA, Jones NP. Evaluation of viscous dampers for stay-cables vibration mitigation. J Bridge Eng 2001;6:385–97.
[12] Weber F, Feltrin G, Motavalli M. Passive damping of cables with MR dampers. J Mater Struct 2005;38(5):568–77.
[13] Johnson EA, Baker GA, Spencer BF, Fujino Y. Semiactive damping of stay cables. ASCE J Eng Mech 2007;133(1):1–23.
[14] Lemura H, Pradono MH. Simple algorithm for semi-active control of cable-stayed bridges. J Earthq Eng Struct Dynam 2005;34(5):409–23.

[15] Cai CS, Wu WJ, Shi XM. Cable vibration reduction with a hung-on TMD system. Part I: Theoretical study. J Vib Control 2006;12(7):801–14.
[16] Wu WJ, Cai CS. Theoretical exploration of a taut cable and a TMD system. J Eng Struct 2006;29:962–72.
[17] Wu WJ, Cai CS. Cable vibration reduction with a hung-on TMD system. Part II: Parametric study. J Vib Control 2006;12(8):881–99.
[18] Casciati F, Ubertini F. Nonlinear vibration of shallow cables with semiactive tuned mass damper. Nonlinear Dynam 2008;53(1–2):89–106.
[19] Main JA, Jones NP. External damping of stay cables using adaptive and semi-active vibration control. In: ICSBOC, the 8th international cable supported bridge operators' conference, Edinburgh, UK; 3–5 June 2013.
[20] Smith MC. Synthesis of mechanical networks: The inerter. IEEE Trans Autom Control 2002;47:1648–62.
[21] Chen MZQ, Papageorgiou C, Scheibe F, Wang F-C, Smith MC. The missing mechanical circuit. IEEE Circ Syst Mag 2009;1531-636X:10–26.
[22] Papageorgiou C, Smith MC. Laboratory experimental testing of inerters. In: 44th IEEE conference on decision and control and the European control conference. Seville, Spain. p. 3351–6.
[23] Papageorgiou C, Houghton NE, Smith MC. Experimental testing and analysis of inerter devices. J Dynam Syst Measur Control, ASME 2009:131.
[24] Wang F-C, Chan H-A. Vehicle suspensions with a mechatronic network strut. Int J Vehicle Mech Mobility 2011;49(5):811–30.
[25] Wang F-C, Liao M-K, Liao B-H, Su W-J, Chan H-A. The performance improvements of train suspension systems with mechanical networks employing inerters. Int J Vehicle Mech Mobility 2009;47:805–30.
[26] Wang F-C, Chen C-W, Liao M-K, Hong M-F. Performance analyses of building suspension control with inerters. In: Proceedings of the 46th IEEE conference on decision and control, New Orleans, LA, USA. p. 3786–91.
[27] Wang F-C, Hong M-F, Chen C-W. Building suspensions with inerters. Proc IMechE, J Mech Eng Sci 2009;224:1605–16.
[28] Ikago K, Saito K, Inoue N. Seismic control of single-degree-of-freedom structure using tuned viscous mass damper. Earthq Eng Struct Dynam 2012;41:453–74.
[29] Ikago K, Sugimura Y, Saito K, Inoue K. Modal response characteristics of a multiple-degree-of-freedom structure incorporated with tuned viscous mass damper. J Asian Architect Build Eng 2012:375–82.
[30] Marian L, Giaralis A. Optimal design of a novel tuned mass-damperinerter (TMDI) passive vibration control configuration for stochastically support-excited structural systems. J Probab Eng Mech 2014. http://dx.doi.org/10.1016/j.probengmech.2014.03.007.
[31] Lazar IF, Neild SA, Wagg DJ. Using an inerter-based device for structural vibration suppression. J Earthq Eng Struct Dynam 2014;43(8):1129–47.
[32] Den Hartog JP. Mechanical vibrations. McGraw Hill; 1940.
[33] Sugimura Y, Goto W, Tanizawa H, Saito K, Nimomiya T. Response control effect of steel building structure using tuned viscous mass damper. In: 15th World conference on earthquake engineering.
[34] Thomson T, Dahleh M. Theory of vibration with applications. Prentice Hall; 1993.
[35] Inman DJ, Singh RJ. Engineering vibration. Prentice Hall; 2001.